Numerical studies of the flame dynamics in a novel, ultra-lean, non-premixed model GT burner using PDF-ESF method

Senbin Yu, Xue-Song Bai,
Department of Energy Sciences, Lund University, Lund, 22100, Sweden
Rajesh Sadanandan
Department of Aerospace Engineering, Indian Institute of Space Science and Technology,
Thiruvananthapuram, Kerala, 695547 India

Abstract

The flame dynamics in a novel, ultra-lean non-premixed model GT burner flame was numerically studied using LES (Large Eddy Simulation) coupled with PDF (Probability Density Function) based on the ESF (Euler stochastic field) method. One non-reacting case and three reacting cases with global equivalence ratio $\phi_{glob} = 1.0, 0.6, 0.3$ were simulated. Comparison of mean flow fields and OH distributions between numerical and experimental results was conducted. Flame dynamics including flame stabilization, structures and transitions of combustion modes were investigated. The simulation results were in close agreement with the experimental measurements showing the PDF-ESF LES model capable of predicting the flame behaviors. At higher ϕ_{glob}, the fuel jet velocity was higher, which yielded higher scalar dissipation rate, χ, near the burner exit, leading to local extinction and flame lifted-off. In the extinction region, a series of low to medium temperature reactions were active, providing favorable conditions for re-ignition downstream where $\chi < \chi_{crt}$. In addition, with ϕ_{glob} decreasing, the flame height decreased due to a smaller jet velocity and χ, and thus the mechanism of flame stabilization changed from the swirl-stabilized to the bluff-body stabilized.

1 Introduction

Combustion takes place in highly turbulent flows in most industrial combustion system, both aero and terrestrial, which makes the stabilization of flames problematic. To mitigate this situation, swirl and bluff-body are generally utilized for the generation of a reversed flow region in real industrial burners [1, 2]. This region, also called re-circulation zone, not only enhances the mixing of fresh fuel with air in a longer residence time, but also provides hot products for the flame stabilization. These burners, running with non-premixed combustion, are widely used attributing to their simpler geometries and better stability. The flames are usually lifted under real conditions as less heat to the burners would prolong their lifetimes. Consequently, flame stabilization of a lifted non-premixed flame is of practical importance to be studied.

Pitts [3] proposed that the lifted flame is stabilized by the balance of flow velocity and turbulent flame speed at a early research. Kelman et al. [4] further clarified that large scale structure entrains ambient air into

Correspondence to: senbin.yu@energy.lth.se, senbinyu@163.com

the flame base, causing local extinction. This extinction extends the mixing time of fuel and air, which results into a partially premixed combustion, further verified by Janus et al. [5]. Lyons [6] reviewed a series of experiments on the lifted jet flame, discussing the effects of partial premixing [7], local extinction [8], large-scale structures [9] and edge flame [10] on the flame stabilization. Despite the great amount work of the turbulent lifted flame, a definitive explanation is not accomplished yet. Additionally, in the presence of re-circulation zones generated by both swirl and bluff-body, the interactions between flow and flame would be extremely complex. Kashir et al. [11] found that a secondary re-circulation zone downstream of the bluff-body induced re-circulation zone would exhibit when swirl number is large enough. Tong et al. [12], in a similar way, claimed that when the bluff-body size is small, the flame would be dominant by the swirl. Recently, Sadanandan et al. [13] described the flame dynamics and stabilization mechanisms. They believed that the flame stabilizes in regions with low velocity and turbulence, though these regions would change under different global equivalence ratio. More studies, however, are still needed to deeply understand the flame dynamics in the presence of bluff-body and swirl.

This paper is a continuation of the previous experimental work [13]. Overall, the objectives of this paper are to 1) validate the combustion model in a non-premixed turbulent flame in the presence of reversed flows induced by swirl and bluff-body; 2) further understand the flame dynamics including the flame stabilization, structures and transitions of combustion modes.

2 Numerical method and setup

Detailed measurement using laser diagnostics on a model GT burner was conducted in a previous study [13]. To further investigate the local extinction and re-ignition phenomena, numerical simulation on the same burner was performed. Large eddy simulation (LES) is a tool more accurate than RANS (Reynolds averaged Navier-Stokes) and more efficient than DNS (Direct numerical simulation), which makes it more suitable for this case with relatively large domain. Smagorinsky model was employed to closure the sub-grid scale motions using

$$\overline{\rho}\tilde{u}_i\tilde{u}_j - \overline{\rho}\widetilde{u_i u_j} = 2\nu_{SGS}\tilde{S}_{ij}, \tag{1}$$

$$\overline{\rho}\tilde{u}_i\tilde{Y}_\alpha - \overline{\rho}\widetilde{u_i Y_\alpha} = \frac{\mu_{SGS}}{\sigma_{SGS}}\frac{\partial \tilde{Y}_\alpha}{\partial x_i}, \tag{2}$$

where $\mu_{SGS} = \overline{\rho}\nu_{SGS}$, $\nu_{SGS} = (C_s\Delta)^2\sqrt{2\tilde{S}_{ij}\tilde{S}_{ij}}$, with $\tilde{S}_{ij}$ being the filtered strain rate tensor, and Y_α denoting the mass fraction of species α. C_s is set to be 0.2 [14] and σ_{SGS} is the turbulent Schmidt/Prandtl number assigned the value of 0.7 [15]. The most challenging term, however, is the source term for the reaction. A transport PDF approach [16] was employed in this paper. Due to the difficulty in solving the PDF equations directly, an ESF method [17, 18] was adopted. The governing equation of $n-th$ stochastic field (ξ_α^n) can be derived as:

$$\overline{\rho}d\xi_\alpha^n = -\overline{\rho}\tilde{u}_i\frac{\partial \xi_\alpha^n}{\partial x_i}dt + \frac{\partial}{\partial x_i}\left[\Gamma_t\frac{\partial \xi_\alpha^n}{\partial x_i}\right]dt + \overline{\rho}\sqrt{2\frac{\Gamma_t}{\overline{\rho}}}\frac{\partial \xi_\alpha^n}{\partial x_i}d\boldsymbol{W}_{\boldsymbol{i}}^n - \frac{\overline{\rho}C_\phi}{2\tau_{SGS}}(\xi_\alpha^n - \tilde{\phi}_\alpha)dt + \overline{\rho}\dot{\omega}_\alpha(\underline{\xi}^n)dt. \tag{3}$$

$\Gamma_t = \mu/\sigma + \mu_{sgs}/\sigma_{sgs}$ denotes the total diffusion coefficient. $d\boldsymbol{W}_{\boldsymbol{i}}^{(n)}$ denotes a Wiener process which is spatially uniform but varying at each field. C_ϕ is a constant representing micro-mixing, chosen to be 2 [15].

The sub-grid mixing time scale is $\tau_{sgs} = \overline{\rho}\overline{\Delta}^2/(\mu + \mu_{sgs})$ [18], and the mean scalar is obtained via

$$\tilde{\phi}_\alpha = \frac{1}{N}\sum_{n=1}^{N}\xi_\alpha^n. \tag{4}$$

By using more stochastic fields, we can obtain more accurate results but with more expensive computation costs. Consequently, 8 stochastic fields [19] were chosen as it is believed that a good balance can be achieved between costs and accuracy. An open source code, OpenFOAM [20] was utilized here solving the equations above. Gauss linear scheme and backward Euler scheme were adopted for the spatial discretization and temporal integration, separately. PISO (pressure implicit with splitting of operator) algorithm was used for solving the pressure-velocity coupling.

In this work, several flames investigated by Sadanandan et al. [13] were simulated. The GT model burner is shown schematically in Fig. 1a. In this burner, a radial swirl consisting of 12 vanes and a broad bluff-body with a height approximately $11mm$ co-exist in the burner to impose swirling motion. At room temperature ($303K$) and pressure ($1bar$), main air flow goes through the radial swirl and issue out through an annular nozzle. The inner and outer diameter are $36mm$ and $42mm$, respectively, leading to a hydraulic diameter of $6mm$ at the nozzle exit. The fuel passes through a non-swirling annular tube with a gap of $0.5mm$ between the wall and bluff-body to issue out. A conical computation domain (cf. Fig. 1b) extending $140mm$ in the downstream direction, $100mm$ in the nozzle exit plane, and $140mm$ in the outlet plane, is adopted for this simulation. Two sets of grid with 3 and 5 million hexahedrons mesh cells are carried out for the mesh insensitivity analyses. For the discussion, the results based on the 5 million grid are employed. As the experiments were conducted in a unconfined environment, free boundary condition is utilized to allow the entrainment of air. Smooke's mechanism with 14 species and 42 reactions was adopted for the chemical reactions, and the critical χ for extinction is $35s^{-1}$ as calculated in Ref. [21].

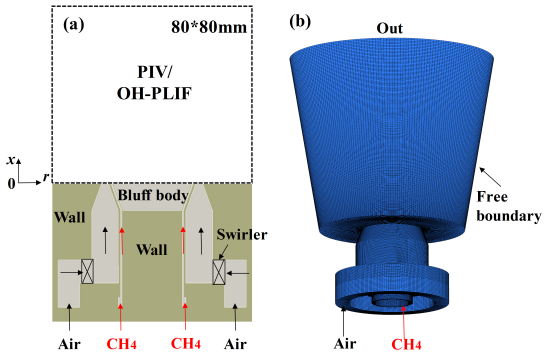

Figure 1: Experimental setup (a) and computation domain.

Four run cases were simulated, including a non-reacting (F1-0), swirl stabilized (F1-1), transition (F1-5) and bluff-body case (F1-8), which are listed in Table 1. In the table Q_{air} and Q_{fuel} represent the air and fuel flow rates, ϕ_{glob} and Z_{glob} represent the global equivalence ratio and mixture fraction, respectively.

3 Results and discussion

Fig. 2 presents the comparison of time-averaged axial velocity from measurement and simulation for non-reacting and reacting case ($\phi_{glob} = 1.0$). The results from the coarse grid (3 million) and the refined grid

Table 1: Case setup and operation conditions

Cases	Q_{air} (slpm)	Q_{fuel} (slpm)	ϕ_{glob}	Z_{glob}
F1-0	100	0	-	-
F1-1	100	10.5	1	0.055
F1-5	100	6.3	0.6	0.034
F1-8	100	3.1	0.3	0.017

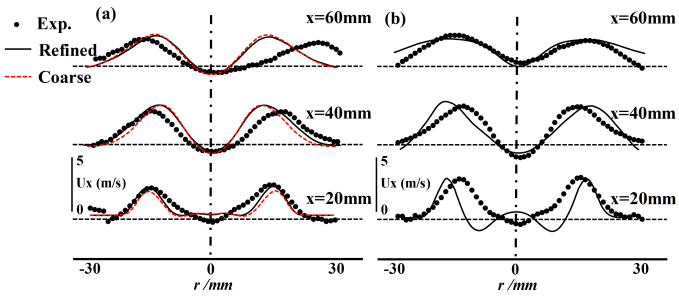

Figure 2: Time-averaged axial velocity comparisons for (a), non-reacting case (F1-0) and (b), swirl stabilized case (F1-1) at varying heights above the burner exit.

(5 million) were compared with each other and it can be inferred that the results are insensitive to the grid as they are quite close. The results from refined grid are chosen for the later analyses and discussions. For F1-0, the simulation matches well with the experimental data, except it shifting a bit compared with the asymmetric data at further downstream. For the reacting case F1-1, the computation results agree well with the measurement except at $x = 20mm$. At this height, it is observed that the simulation over-predicts the two isolated re-circulation zones while these two zones are combined as an intact structure in the measurements. Overall, the trends and shapes are reasonably well captured by the LES-PDF method implying that this method is suitable for this case.

Fig. 3 illustrates the instantaneous distributions of CH_2O, OH, temperature, heat release rate (HRR), scalar dissipation rate χ and axial velocity U_x. In this figure, white line denotes the stoichiometric mixture fraction $Z_{st} = 0.055$, green line denotes the iso-line of CO_2 with the value of 0.06 (mass fraction). For F1-1, the OH region is lifted-off above $x = 40mm$ and has a divergent shape. Note that OH mostly distributes along the Z_{st} line, but at the base, OH occurs at both rich and lean side, implying an edge flame. CH_2O is abundant upstream of OH with relatively lower temperature, which indicates that low temperature reactions take place there giving rise to the formation of radicals for the flame stabilization downstream. HRR coincides well with the iso-line of $Y_{CO_2} = 0.06$. High χ is found near the burner exit and the shear layer, which prohibits the flame and leads to the local extinction. It is also noted from its axial velocity that, a convergent re-circulation zone is induced by the bluff-body and a divergent zone is induced by the swirl. With the decreasing fuel jet velocity, the flame height of F1-5 reduces and the flame stabilization position is moved from the swirl stabilized re-circulation zone to the transition zone. The flame shape keeps slim under the combined effects of swirl and bluff-body. Furthermore, for F1-8, the flame shrinks within the re-circulation zone induced by the bluff-body and stabilizes at the low χ region. It is conclusively seen that with decreasing fuel jet velocity, the mechanism of flame stabilization is changed from the swirl stabilized to the bluff-body stabilized one, with the leading flame front moving closer to the burner exit.

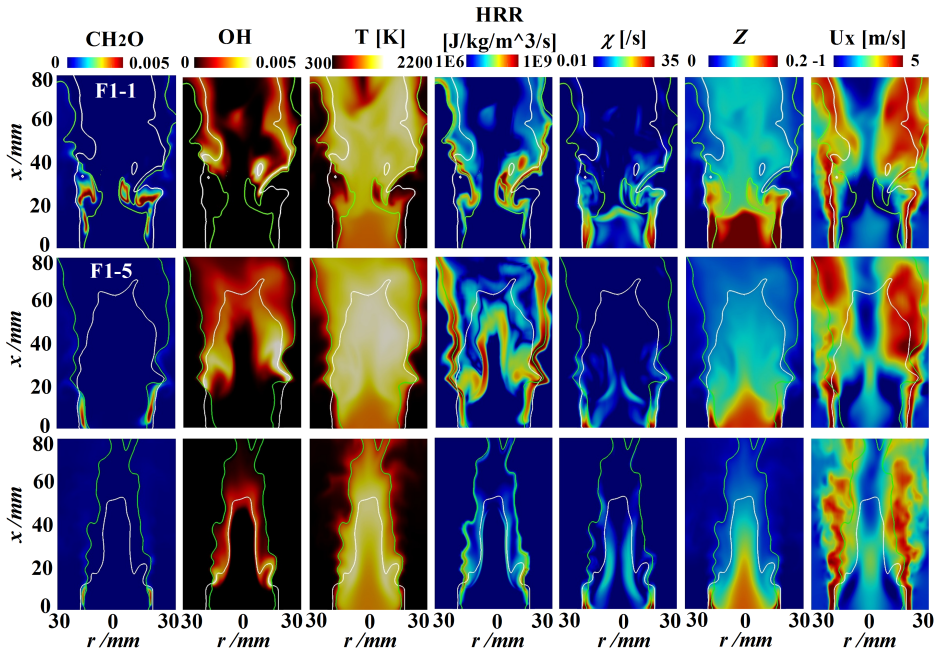

Figure 3: Instantaneous scalar fields of CH_2O, OH, T, HRR, χ and U_x. White line represents the stoichiometric mixture fraction $Z_{st} = 0.055$, green line represents the iso-line of CO_2 with the value of 0.06 (mass fraction)

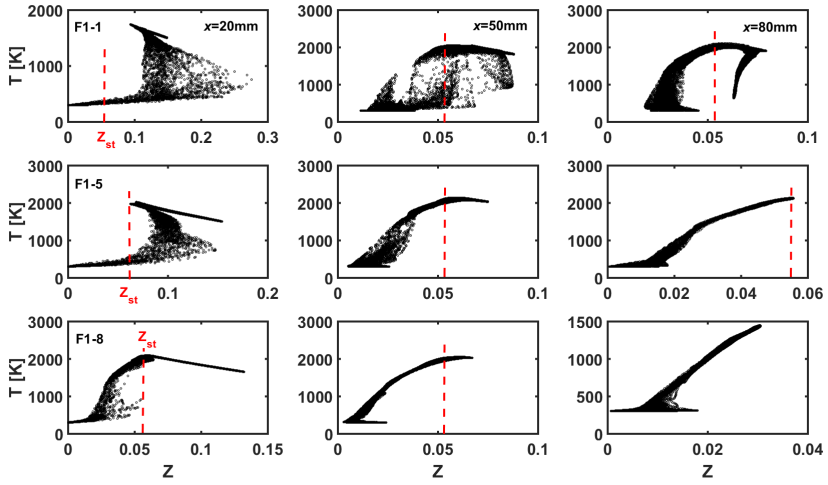

Figure 4: Temperature distributions in the mixture fraction space at three heights for different combustion modes. Red line denotes the stoichiometric mixture fraction

Fig. 4 demonstrates the temperature distributions in the mixture fraction space for three cases at varying heights. For all the cases, with the growing height, Z decreases rapidly as more air is mixed with the fuel. For F1-1, the temperature scatters in a wide range around $1000K$ at $x = 20mm$ under fuel-rich condition ($Z > Z_{st}$) implying an ignition mode of combustion in these mixtures. At further downstream, $x = 50mm$, T peaks around Z_{st}, but the temperature scatters in both the lean and the rich mixtures, implying the ongoing ignition process in these mixtures. At $80mm$ the temperature falls into a manifolds implying the establishment of diffusion flame front. For F1-8, on the contrary, a diffusion flame front is already formed at $x = 20mm$, close to the burner exit and stabilizes in the bluff-body re-circulation zone. With the further increases of height, e.g. at $80mm$, the entire mixture is fuel-lean ($Z < Z_{st}$), owing to the ambient air mixing to the flame. Thereafter T decreases because the entrained ambient air cools the hot gas formed upstream. For F1-5, T shows a similar trend with F1-1 in rich mixture ignition mode at $x = 20mm$ though a higher temperature manifolds appears here. Further downstream, at $x = 50$ and $80mm$, temperature keeps high around Z_{st} indicating a diffusion flame front, which is similar to the case F1-8. The flame stabilization of F1-5 is highly affected by both the swirl and bluff-body induced recirculating flows.

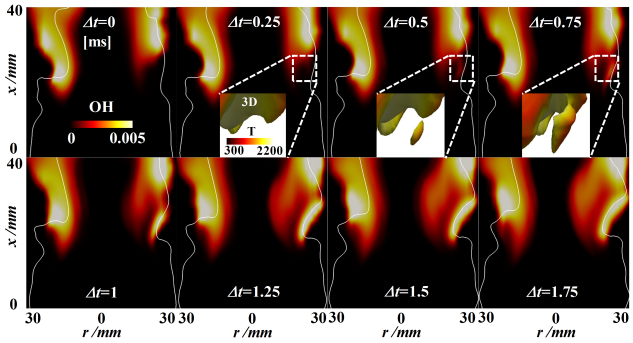

Figure 5: The dynamic process of case F1-5 in a transition mode. White lines denote the stoichiometric mixture fraction and 3D contours correspond to $Y_{OH} = 0.02$ (mass fraction)

Fig. 5 illustrates the dynamic process of flame kernels using OH to denote the flame front for case F1-5. The flame front as marked by OH distributes in both rich and lean side, which implies the characteristics of edge flame. In this case, the flame is controlled by both the swirl and bluff-body, stabilizing in a transition region. After a time interval of $\Delta t = 0.5ms$, an isolated flame kernel occurs upstream the flame front. This is also confirmed in 3D iso-contour (shown in the inset of Fig. 5) to take into account of the out-of-plane effects. After $\Delta t = 0.75ms$, this flame kernel combines with the main flame, causing the flame front propagating upstream into the bluff-body induced re-circulation region. Afterwards, due to the existence of high scalar dissipation rate there, it is gradually quenched (OH intensity weakens), which leads to the flame front propagating downstream again. It is thus believed that the quenching and re-ignition occurs repeatedly, which means that the flame in this transition region will move between swirl-stabilized and bluff-body stabilized region dynamically. Additionally, the OH flame front propagates along the stoichiometric lines, indicating an edge flame propagation mode.

4 Conclusion

LES coupled with PDF-ESF method was employed to simulate the flame dynamics (including flame stabilization, structures and transitions of combustion modes) in a novel, ultra-lean non-premixed model GT burner. Several findings were concluded as follows:

- The PDF-ESF combustion model in the framework of LES can capture the multiple combustion modes in a complex flow field, with the mean flow structures in satisfactory agreement with experimental results.
- A higher ϕ_{glob} produces higher scalar dissipation rate near the burner exit, leading to the local extinction and thus flame lifted-off. The mixture upstream the flame front is shown to undergoing ignition reaction that gives rise to a wide scattering of temperature with relatively heat release rate, first in the fuel-rich side of the mixture and later in both the lean and rich mixtures. These ignition reactions trigger the onset of high temperature ignition and the establishment of diffusion flame downstream in the swirl-induced recirculation zone.
- With decreasing ϕ_{glob}, the flame is transferred from the swirl-stabilized to the bluff-body stabilized mode, with decreasing flame height. Specifically, the $\phi_{glob} = 1.0$ flame is mostly governed by the swirl stabilization mechanism, while the $\phi_{glob} = 0.3$ flame is mostly controlled by the bluff-body stabilization mechanism, whereas the $\phi_{glob} = 0.6$ is a transition case which is dominant by both the swirl and bluff-body.

Acknowledgments

This work was partly sponsored by Swedish Research Council (VR), and the Swedish Energy Agency (STEM) through the national center for combustion science and technologies (CeCOST). Senbin Yu was sponsored by China Scholarship Council (CSC).

References

[1] H. I. Saravanamuttoo, G. F. C. Rogers, H. Cohen, Gas turbine theory, Pearson Education, 2001.

[2] Y.-C. Chen, C.-C. Chang, K.-L. Pan, J.-T. Yang, Flame lift-off and stabilization mechanisms of nonpremixed jet flames on a bluff-body burner, Combustion and flame 115 (1-2) (1998) 51–65.

[3] W. Pitts, Assessment of theories for the behavior and blowout of lifted turbulent jet diffusion flames, Proc. Combust. Inst. 22 (1988) 809–816, cited By 55.

[4] J. B. Kelman, A. J. Eltobaji, A. R. Masri, Laser imaging in the stabilisation region of turbulent lifted flames, Combustion Science and Technology 135 (1-6) (1998) 117–134.

[5] B. Janus, A. Dreizler, J. Janicka, Experimental study on stabilization of lifted swirl flames in a model GT combustor, Flow, turbulence and combustion 75 (1-4) (2005) 293–315.

[6] K. M. Lyons, Toward an understanding of the stabilization mechanisms of lifted turbulent jet flames: experiments, Progress in Energy and Combustion Science 33 (2) (2007) 211–231.

[7] V. Favier, L. Vervisch, Edge flames and partially premixed combustion in diffusion flame quenching, Combustion and flame 125 (1-2) (2001) 788–803.

[8] F. Takahashi, W. J. Schmoll, D. D. Trump, L. P. Goss, Vortex-flame interactions and extinction in turbulent jet diffusion flames, in: Symposium (International) on Combustion, Vol. 26, Elsevier, 1996, pp. 145–152.

[9] R. C. Miake-Lye, J. A. Hammer, Lifted turbulent jet flames: a stability criterion based on the jet large-scale structure, in: Symposium (International) on Combustion, Vol. 22, Elsevier, 1989, pp. 817–824.

[10] J. Buckmaster, Edge-flames, Progress in Energy and Combustion Science 28 (5) (2002) 435–475.

[11] B. Kashir, S. Tabejamaat, N. Jalalatian, A numerical study on combustion characteristics of blended methane-hydrogen bluff-body stabilized swirl diffusion flames, International journal of hydrogen energy 40 (18) (2015) 6243–6258.

[12] Y. Tong, X. Liu, Z. Wang, M. Richter, J. Klingmann, Experimental and numerical study on bluff-body and swirl stabilized diffusion flames, Fuel 217 (2018) 352–364.

[13] R. Sadanandan, A. Chakraborty, V. K. Arumugam, S. R. Chakravarthy, Optical and laser diagnostic investigation of flame stabilization in a novel, ultra-lean, non-premixed model GT burner, Combustion and Flame 196 (2018) 466–477.

[14] C. Leith, Stochastic backscatter in a subgrid-scale model: Plane shear mixing layer, Physics of Fluids A: Fluid Dynamics 2 (3) (1990) 297–299.

[15] W. Jones, V. Prasad, Large eddy simulation of the Sandia Flame Series (D–F) using the Eulerian stochastic field method, Combustion and Flame 157 (9) (2010) 1621–1636.

[16] S. B. Pope, PDF methods for turbulent reactive flows, Progress in energy and combustion science 11 (2) (1985) 119–192.

[17] L. Valiño, A field Monte Carlo formulation for calculating the probability density function of a single scalar in a turbulent flow, Flow, turbulence and combustion 60 (2) (1998) 157–172.

[18] R. Mustata, L. Valiño, C. Jiménez, W. Jones, S. Bondi, A probability density function Eulerian Monte Carlo field method for large eddy simulations: application to a turbulent piloted methane/air diffusion flame (Sandia D), Combustion and Flame 145 (1-2) (2006) 88–104.

[19] M. Jangi, M. Altarawneh, B. Z. Dlugogorski, Large-eddy simulation of methanol pool fires using an accelerated stochastic fields method, Combustion and Flame 173 (2016) 89–98.

[20] H. Jasak, OpenFOAM: open source CFD in research and industry, International Journal of Naval Architecture and Ocean Engineering 1 (2) (2009) 89–94.

[21] A. M. Elbaz, S. Yu, X. Liu, X. Bai, I. Khesho, W. L. Roberts, An experimental/numerical investigation of the role of the quarl in enhancing the blowout limits of swirl-stabilized turbulent non-premixed flames, Fuel 236 (2019) 1226–1242.